Hydrology Research

Hydrology Research Vol 54 No 4, 508 doi: 10.2166/nh.2023.096

Distribution characteristics and influencing factors of water resources in Henan Province

Yishuang Zhou[a], Xiaoxia Tong[b,*], Rong Gan[a,c], Panfeng Liu[d], Lin Guo[e] and Shanshan Zhao[f]

[a] School of Water Conservancy Engineering, Zhengzhou University, Zhengzhou 450001, China
[b] China Geological Environmental Monitoring Institute, Beijing 100081, China
[c] Henan Key Laboratory of Groundwater Pollution Prevention and Rehabilitation, Zhengzhou 450001, China
[d] No. 1 Institute of Geo-Environment Survey of Henan, Zhengzhou, China
[e] Henan Institute of Geology Survey, Zhengzhou, China
[f] Henan Baoyuan Exploration Technology Co., Ltd, Zhengzhou, China
*Corresponding author. E-mail: ktz2022@163.com

ABSTRACT

A clear understanding of the spatial and temporal distribution characteristics of water resources is essential for the optimal allocation and sustainable utilization of water resources. In this paper, the spatial and temporal distribution characteristics of water resources in Henan Province were studied based on GIS, combining the Mann-Kendall (M-K) nonparametric test and rescaled range (R/S) analysis. In addition, SPSS software was used to analyze the influence of climate and land use type on water resources. The results indicated that (1) the hot spots of water resources were concentrated in the southwest, while the low values were concentrated in the northeast, and the distribution of water resources decreased from southwest to northeast. (2) In the past 21 years, spatiotemporal mutations in the water resource sequence occurred between 2010 and 2014. The *Z*-values of the M-K trend test were all less than 0, the *H*-values of groundwater resources (GWRs) were mostly greater than 0.5, and the *h*-values of surface water resources (SWRs) and total water resources (TWRs) were less than 0.5, showing an overall declining trend. However, this trend may change in the future. (3) From the correlation analysis, climate change had a greater impact on water resources than land use changes did.

Key words: GIS, interannual variation, Mann-Kendall, regional distribution, R/S analysis, water resources

HIGHLIGHTS

- Combining the M-K method and R/S analysis to study water resource sequences and used GIS to visualize the analysis.
- Both temporal and spatial characteristics of water resources had abrupt changes during the 21 years, and they occurred at similar times. Precipitation had a greater effect than temperature on water resources, while land use had no significant effect on water resources.

GRAPHICAL ABSTRACT

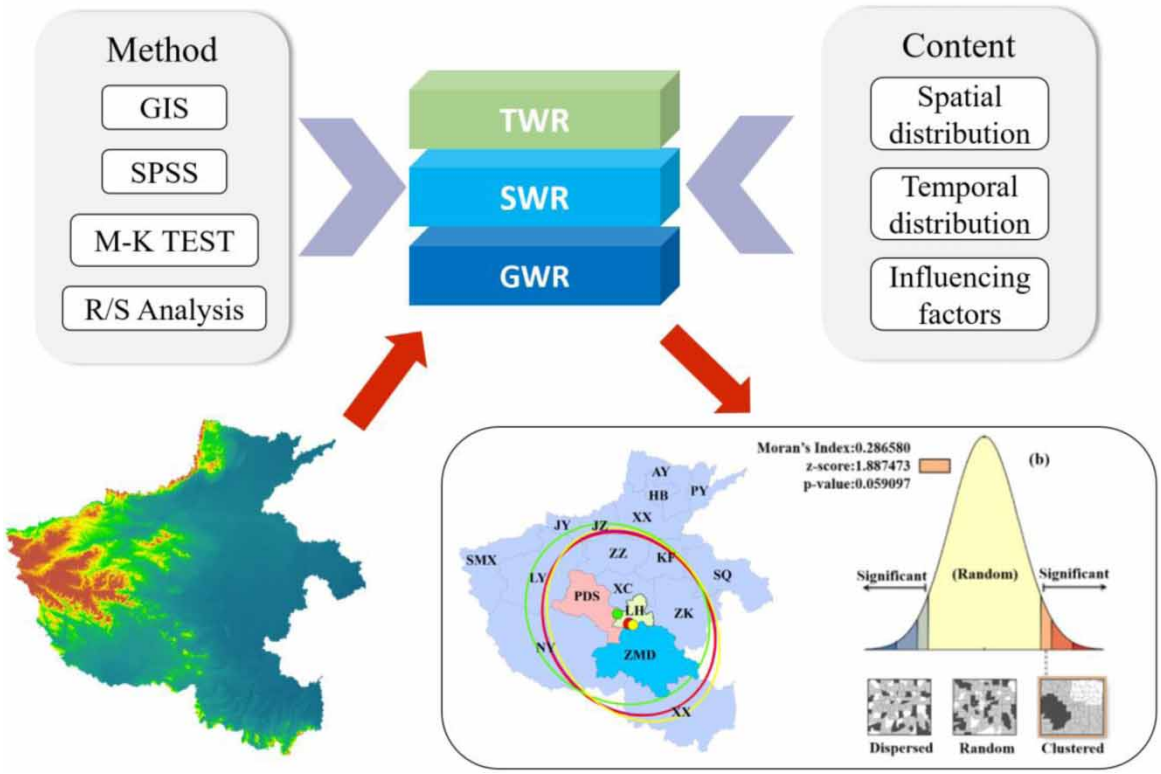

INTRODUCTION

Water is an important raw material for industrial and agricultural production, is a valuable natural resource needed for human survival, and is closely related to the ecological cycle and human economic activities. Water resource shortages are not only a serious problem in the world but also an important factor related to a country's national livelihood and sustainable economic development (Li *et al.* 2019; Zuo *et al.* 2020). It is necessary to study the spatial and temporal distributions of water resources, but there is almost no relevant research in Henan Province. In addition, at present, almost all research on water resources in Henan Province has been carried out from a single aspect and thus lacks a comprehensive analysis from multiple perspectives.

As a country with severe water shortages, the situation is even worse in western and northern China, and the total water resources are unevenly distributed among provinces (Song *et al.* 2018). Located in Central China, Henan Province is the only province of the country that straddles four major river basins: the Yangtze River, the Huai River, the Yellow River, and the Hai River, and its water resource distribution is considered to be a microcosm of China and is representative of the country. In northern China, where water resources are generally scarce, Henan Province has average water resources of 440 m^3/capita, equivalent to one-sixth of the national level, which indicates the province has a serious water shortage. In addition, the situation of water resources in Henan Province is very worrying because of its low utilization rate, serious waste, and pollution (Wang *et al.* 2021). According to the Henan Water Resources Bulletin, the total amount of water resources in 2019 was 16.89 billion m^3, which was 58.1% lower than the long-term average annual value and 50.3% lower than that in 2018. The province's precipitation was 529.1 mm in 2019, which was 29.9% less than that in 2018 and 31.4% less than the long-term average annual value. It is estimated that by 2025, under the 95% guarantee rate, the water shortage in Henan Province will reach 2.211 billion m^3 (Zhou 2014). The water resources in Henan Province have the characteristics of uneven spatial and temporal distributions, concentrated annual distributions of precipitation and river runoff, and large annual variability (Zhang *et al.* 2020). For this current situation, some scholars have also studied the interbasin water resource allocation scheme in Henan Province, evaluated the coupled water–energy–food system, and determined the status of groundwater overdraft (Liu *et al.* 2020; Du & Song 2021; Yu *et al.* 2021). Some relevant studies have been published, such as Gu *et al.*'s (2010)

analysis of the variation characteristics of precipitation and water resources in Henan Province from 1956 to 2007, and they evaluated the abundance and depletion of the water resource quantity. However, there have been few detailed studies on the spatiotemporal changes in water resources in Henan Province in recent years. In this context, it is necessary to study the spatial and temporal distributions of water resources in Henan Province and its influencing factors, which can support the optimal allocation of water resources and provide recommendations for sustainable water resource use, thus alleviating the increasingly severe water resources in Henan Province.

Water resources can be affected by climate and anthropogenic activities, such as precipitation, temperature, dam construction, consumptive use, and agricultural irrigation (Wang *et al.* 2020). They can affect water resources on temporal and spatial scales by influencing processes such as the hydrological cycle. To solve the problem of water scarcity caused by agricultural activities and climate fluctuations, Rahmani & Danesh-Yazdi (2022) studied the impact of different patterns on water resources. Man-made pollution affects precipitation and runoff, impairs water quality, and reduces available water resources (Khan *et al.* 2017, 2020). However, most of the studies on the influencing factors of water have focused mainly on the hydrological process, such as the simulation of the change or composition of the water cycle in future land use and climate scenarios (Freund *et al.* 2017), the sustainability of water resources (Bhatti *et al.* 2021), and the influence of reservoirs on runoff (Zhao *et al.* 2021), while research on the influencing factors of water resources is scarce.

Since hydrological time series have fractal characteristics and generally do not obey a normal distribution, a nonparametric statistical method is often used for trend analysis in hydrology (Yang *et al.* 2017). The Mann-Kendall (M-K) method focuses on analyzing the trend of time series in a certain time period and detecting mutations from a quantitative perspective; however, this method cannot predict future trends. Rescaled range analysis (R/S) focuses on analyzing the fractal characteristics of time series in the future from a qualitative perspective, which can better reveal whether the future trend is the same as the past trend (Qi 2019).

To expand the research on the quantity of water resources and provide data support for the planning and allocation of water resources, the following research was carried out. The main objectives of this study were to analyze the spatiotemporal variation characteristics of water resources in Henan Province from 1999 to 2019 and predict the future trend of water resource change. Moreover, the impacts of climate and land use types on water resources are discussed.

STUDY AREA AND DATA

The study area, which was in Henan Province, is shown in Figure 1. It is located in Central China, bounded between 31°23′–36°22′N and 110°21′–116°39′E. With a total area of 167,000 km^2, the terrain is high in the west and low in the east, and the highest elevation is 2,413.8 m and the lowest is only 23.2 m. The central and eastern parts of Henan Province are plains, with mountains in the north, west and south along the provincial boundary in a semicircular distribution. The average annual water resources in Henan Province are 40.353 billion m^3, and the per capita water resources is about 368 m^3, which is less than 1/5 of the national level and indicates a serious water shortage. Most of Henan Province is in the warm temperate zone, and the southern part crosses the subtropical zone, which is a continental monsoon climate with the transition from the northern subtropical zone to the warm temperate zone. The annual average temperature of the province in the last 10 years was 12.9–16.5 °C, and the annual average precipitation was 464.2–1,193.2 mm, with the most rainfall occurring from June to August. The changes of precipitation and temperature in the study area during 1999–2019 are shown in Figure 2 (precipitation: mm and temperature: °C).

The study was based on 17 cities in Henan Province: Zhengzhou (ZZ), Kaifeng (KF), Luoyang (LY), Pingdingshan (PDS), Anyang (AY), Hebi (HB), Xinxiang (XX), Jiaozuo (JZ), Puyang (PY), Xuchang (XC), Luohe (LH), Sanmenxia (SMX), Nanyang (NY), Shangqiu (SQ), Zhumadian (ZMD), and Jiyuan (JY).

Data and sources

This paper mainly used the annual data of water resources in Henan Province over the past 21 years, which came from the Bulletin of Water Resources in Henan Province from 1999 to 2019 (http://slt.henan.gov.cn/bmzl/szygl/szygb/). Water resources were divided into SWR, GWR, and TWR for research. The geographic situation data of the study area were from the Henan People's Government website (https://www.henan.gov.cn/), the 30 m precision DEM data were from the Geospatial Data Cloud (http://www.gscloud.cn/), the precipitation and temperature data were from the Henan

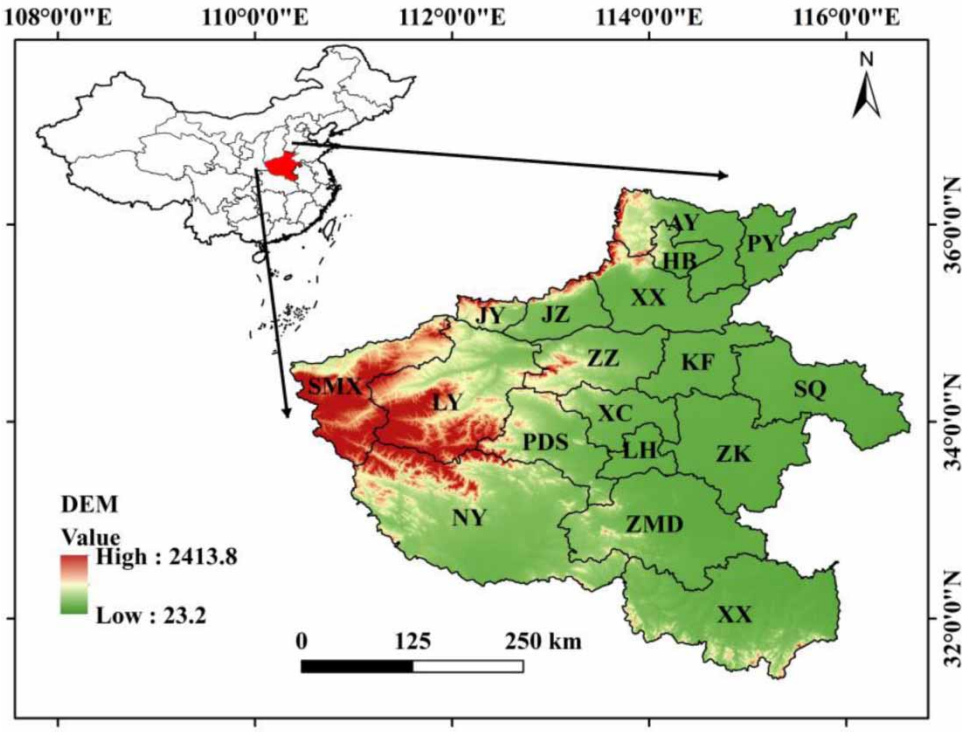

Figure 1 | Schematic diagram of the study area.

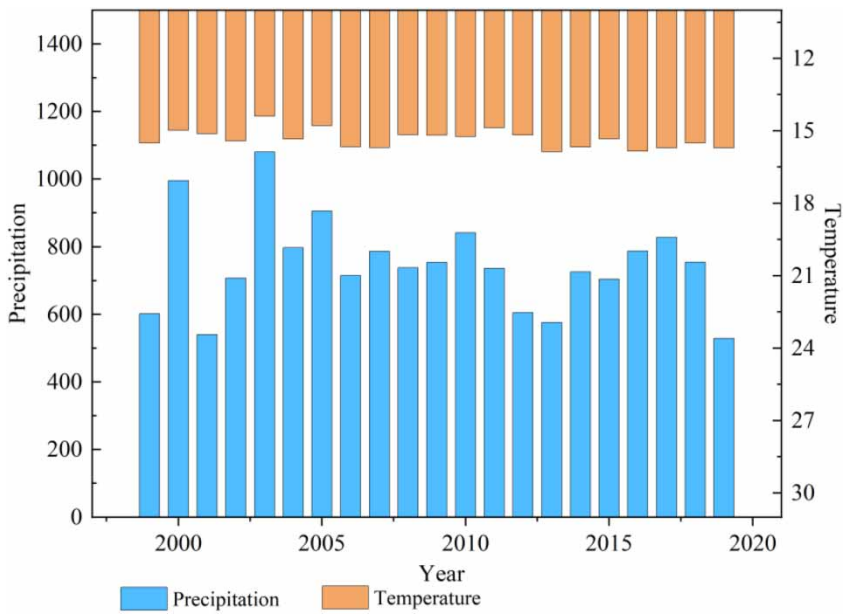

Figure 2 | Precipitation and temperature changes in the study area.

Water Resources Bulletin and China Meteorological Data Network, respectively, and the land use data with a resolution of 300 m were from the European Space Agency and Copernicus Climate Change Service (http://maps.elie.ucl.ac.be/CCI/viewer/).

METHODS

The flowchart of the main research methods used in this paper and its contents is shown in Figure 3.

Geographic information system

A geographic information system (GIS) is a data system that can collect, manage, and analyze spatial attribute data and organize and visualize data rationally in computer space (Deng *et al.* 2020). This paper realized the visual processing and spatial statistical analysis of data and mapping with the help of ArcGIS tools.

1. Measuring geographic distribution. The mean center, median center, center feature, and directional distribution tools were used in this paper for the analysis. The mean center identifies the geographic center or density center of a group of elements. The central feature is the most centrally located element among point, line, or polygon features. Standard deviation ellipses (SDEs) are created in the directional distribution to summarize the spatial characteristics of geographic elements; one SDE contains approximately 63% of the elements in the cluster, two contain approximately 98%, and three contain approximately 99%. In SDE, the directions of its long and short axes indicate the primary and secondary trend directions of geographic elements distributed in space, and the lengths indicate the dispersion of geographic elements in the corresponding directions (He *et al.* 2021).
2. Moran's I. The Spatial Autocorrelation (Global Moran's I) tool measures spatial autocorrelation based on both feature locations and feature values simultaneously. Given a set of features and an associated attribute, this tool evaluates whether the expressed pattern is clustered, dispersed, or random. This tool evaluates the significance of that index by calculating the Moran's I index, *p*-value, and *z*-score, where the *p* is the significance level, limited by the test statistic. The Global Moran's I

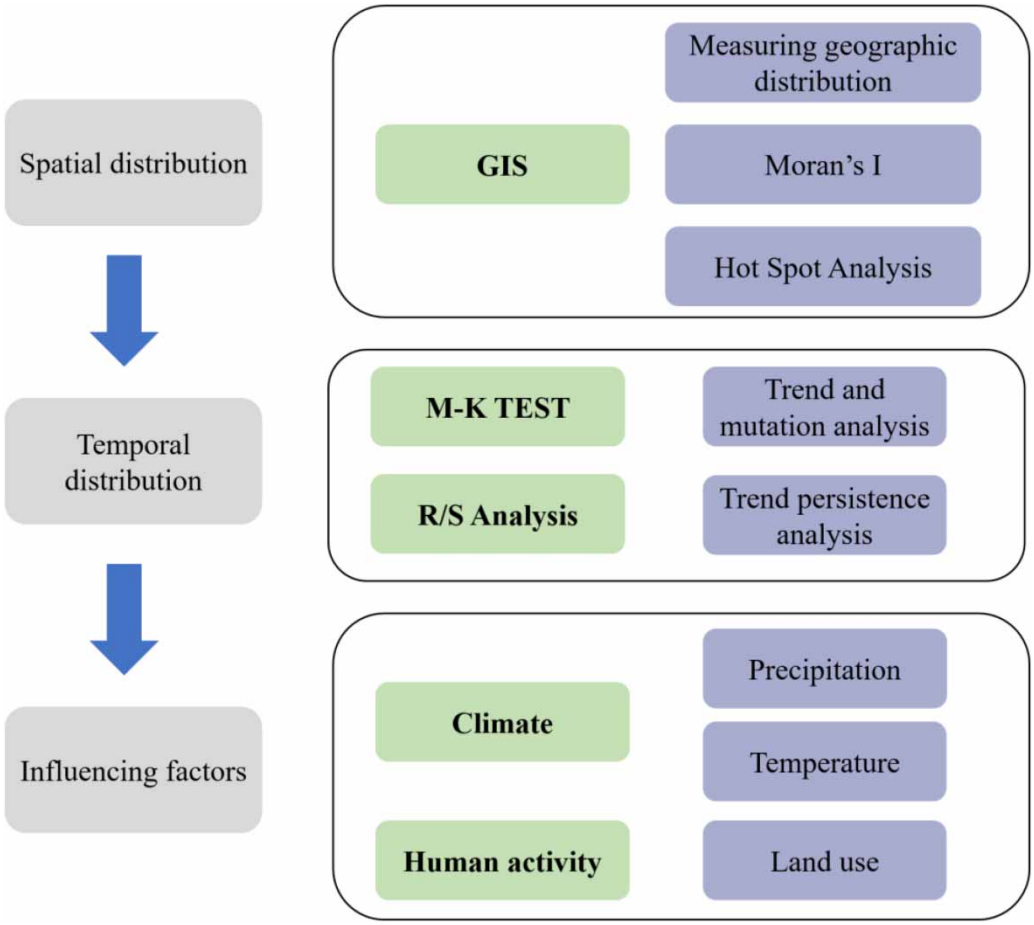

Figure 3 | Flowchart of the methodology.

ranges from −1 to 1. When it is greater than 0, the data are spatially positively correlated, and values less than 0 are negatively correlated; otherwise, the space is random. It should be noted that even if the Global Moran's I is 0, local spatial aggregation cannot be excluded on this basis, and the Cluster and Outlier Analysis (Local Moran's I) tool was used to further analyze the spatial clusters of features with high or low values. Additionally, Local Moran's I can identify spatial outliers.

3. Hot Spot Analysis. The Hot Spot Analysis tool calculates the Getis-Ord Gi* statistic for each feature in a dataset to obtain the *z*-scores and *p*-values. These indices reflect where features with either high or low values are clustered spatially. The data were combined with Moran's I to assess the statistical characteristics of water resources in Henan Province.

M-K nonparametric test

The M-K nonparametric method is recommended and widely used by the World Meteorological Organization for trend analysis and mutation detection of sequences (Zhang *et al.* 2015), and it is based on the following principles (Wei 2007).

For the trend test, the null Hypothesis H_0 is proposed, which states that the time series $\{x_1, x_2, \ldots, x_n\}$ are n independent and identically distributed random variables, and the alternative Hypothesis H_1 holds that x_i and x_j have different distributions for all $i, j \leq n$, and $i \neq j$. The test statistic S is defined as follows:

$$S = \sum_{i=2}^{n} \sum_{j=1}^{i-1} \text{sign}(X_i - X_j) \tag{1}$$

where sign () is a symbolic function with the following meaning:

$$\text{sign}(X_i - X_j) = \begin{cases} 1, & X_i > X_j \\ 0, & X_i = X_j \\ -1, & X_i < X_j \end{cases} \tag{2}$$

The variance of S is as follows:

$$\text{Var}(S) = n(n-1)(2n+5)/18 \tag{3}$$

The value of the test statistic Z is taken as follows:

$$Z = \begin{cases} (S-1)/\sqrt{\text{Var}(S)}, & S > 0 \\ 0, & S = 0 \\ (S+1)/\sqrt{\text{Var}(S)}, & S < 0 \end{cases} \tag{4}$$

In the two-tailed test, for a given confidence level α, the statistic Z is calculated, rejecting H_0 and accepting H_1 if $|Z| \geq Z_{1-\alpha/2}$. Therefore, there is a significant upward or downward trend of the time series data at the confidence level α. $Z > 0$ indicates an upward trend, and $Z < 0$ indicates a downward trend. When $|Z|$ is greater than or equal to 1.64, 1.96, and 2.58, it means that the significance test with 90, 95, and 99% confidence levels is passed, respectively.

For abrupt analysis, it is necessary to construct the sequence S_k, where S_k denotes the cumulative count of the ith sample $x_i \geq x_j$:

$$S_k = \sum_{i=1}^{k} r_i \tag{5}$$

$$\text{where } r_i = \begin{cases} 1, x_i > x_j \\ 0, x_i < x_j \end{cases}, \quad (j = 1, 2, \ldots, i;\ k = 1, 2, \ldots, n)$$

The statistic UF_k is defined as follows:

$$UF_k = \frac{(S_k - E[S_k])}{\sqrt{Var[S_k]}} \tag{6}$$

where the expectation and variance of S_k are: $E[S_k] = k(k-1)/4$, $Var[S_k] = k(k-1)(2k+5)/72$, and $UF_1 = 0$.

UF_k' was obtained in the same way using the inverse series data x_n, $x_{(n-1)}$, …, x_1 so that $UB_k = -UF_k$ where $UB_1 = 0$. For a given significance level $\alpha = 0.1$ and a critical value $U_\alpha = 1.64$, the UF_k and UB_k curves and $\pm$ 1.64 straight lines are plotted on the same graph, and if an intersection occurs and the intersection is between the critical lines, then the intersection is the mutation point, and its corresponding time is the time when the mutation starts.

R/S analysis

The rescaled range (R/S) analysis method was originally a time series statistical method proposed by the hydrologist Hurst in 1965 while studying Nile dams (Ye *et al.* 2018). Currently, it has been applied in many research fields, such as hydrology and ecology, and is usually used to study the fractal characteristics of time series and long-term memory processes (Peng *et al.* 2012; Xiao *et al.* 2019). Based on the research of Peng and Xiao, the principle of R/S analysis is as follows:

For a time series $\{x_i\}$, $i = 1, 2, \ldots, N$.

1. Divide the series into n subintervals of length t. The elements in each subinterval are denoted as $T_{i,j}$, $i = 1, 2, \ldots, n$; $j = 1, 2, \ldots, t$. Calculate the mean value of each subinterval.

$$\overline{m_i} = \frac{1}{t}\sum_{j=1}^{t} T_{i,j} \tag{7}$$

2. Calculate the cumulative deviation of each subinterval element from its corresponding mean and then obtain the range:

$$D_{i,k} = \sum_{j=1}^{k} (T_{i,j} - \overline{m_i}) \tag{8}$$

This yields the polar difference R_i for each subinterval, defined as follows:

$$R_i = \max D_{i,k} - \min D_{i,k} \tag{9}$$

where $k = 1, 2, \ldots, t$, $i = 1, 2, \ldots, n$.

3. The standard deviation of each set of subintervals is as follows:

$$S_i = \sqrt{\frac{1}{t}\sum_{j=1}^{t} (T_{i,j} - \overline{m_i})^2} \tag{10}$$

4. Calculate the Hurst exponent (H):

$$\frac{R(n)}{S(n)} = C(n)^H \tag{11}$$

where H is the Hurst exponent, and $R(n)$ and $S(n)$ are the Ri and Si sequences, respectively. By taking the logarithms of both sides of the above equation simultaneously, we can obtain the following equation:

$$\lg \frac{R(n)}{S(n)} = \lg C + H \lg n \tag{12}$$

The slope of the regression line is the value of the Hurst index when lg $(R(n)/S(n))$ and lg n are plotted, and linear regression analysis is performed using the least squares method. When $H = 0.5$, the time series is considered to be independently distributed, that is, the past trend of change has no effect on the future; when $0 < H < 0.5$, it means that the series has inverse persistence, that is, the future trend of change is opposite to the past; when $0.5 < H \leq 1$, it means that the series has persistence, that is, the future trend of change is the same as the past. In addition, the more H tends to 0, the stronger the inverse persistence is, and conversely, the more H tends to 1, the stronger the persistence is.

RESULTS AND DISCUSSION

Spatial variation characteristics of water resources

Water resources in the south are obviously more abundant than those in the north, and the water resources in the southeast, represented by several cities such as Xinyang and Zhumadian, always occupy a larger proportion. The spatial variation in the multiyear average water resources in each city is shown in Figure 4(a). The results of the analysis using the measurement geographic distribution tool are shown in Figure 3, where point, line, and polygon represent the mean center, SDE, and central feature, respectively. From the perspective of multiyear average water resources (Figure 4(a)), the direction distributions of SWR and TWR were similar, showing a northwest–southeast distribution, and the mean centers were concentrated at the

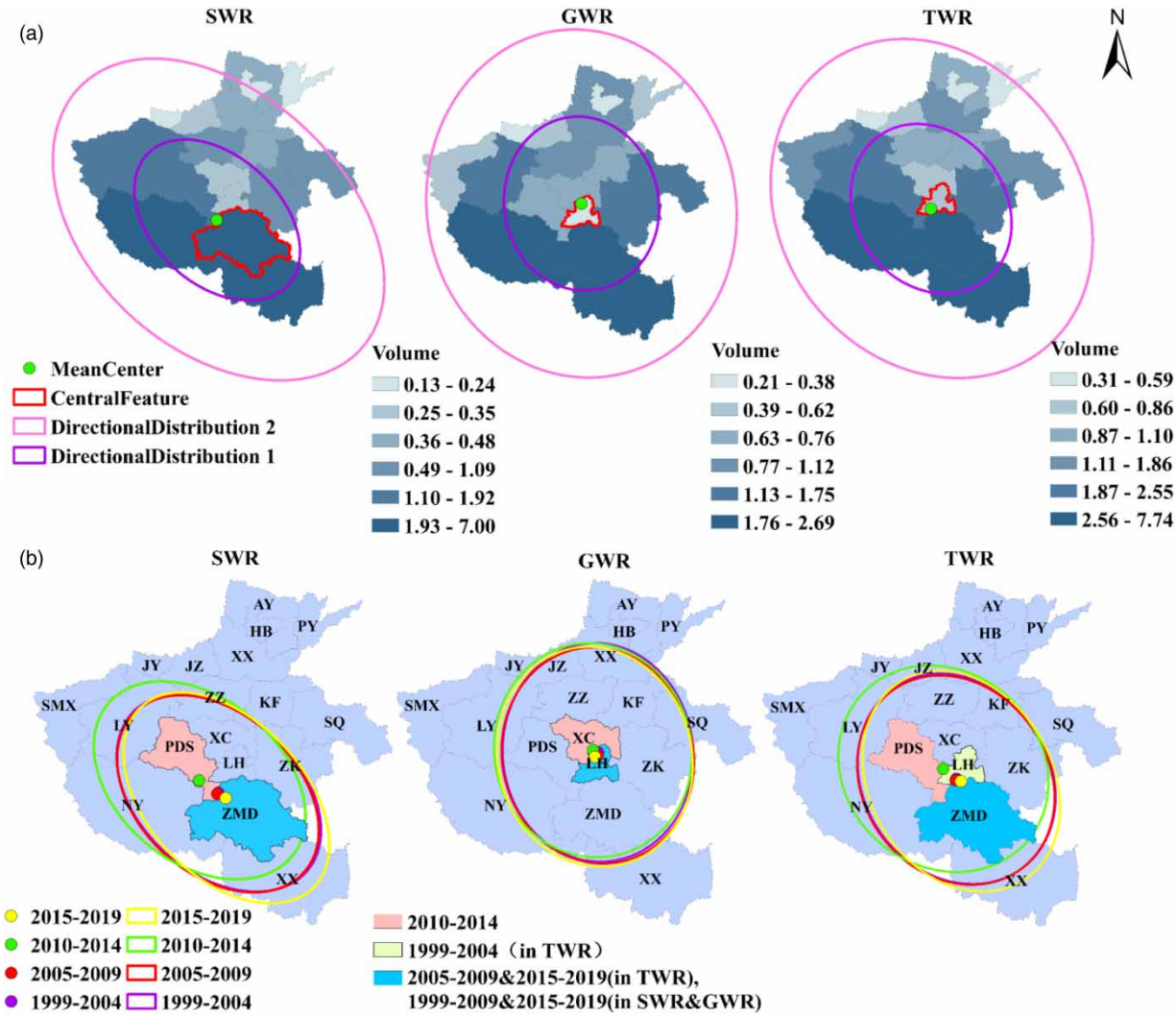

Figure 4 | (a) Spatial variation of water resources in Henan Province (unit of water resource volume: billion m^3) and (b) Geographical distribution of water resources by time period.

junction of PDS, LH, and ZMD. However, SWR's central feature was located in ZMD, while TWR's was located in LH. Comparatively speaking, the direction distribution of GWR was mainly north–south, and the mean center moved slightly north, located at the junction of LH and XC, and the central feature was located in LH.

The next step is to divide the data into four time periods and calculate the average value of that time period, as shown in Table 1. The change in spatial characteristics over time is shown in Figure 4(b). GWR indicated no significant changes in the SDE and the mean center, but the central feature shifted from the previous LH to XC in 2010–2014, and then returned to LH after 2014. The changes in SWR and TWR were similar, with no significant change in the shape of the SDE, but its position shifted significantly in 2010–2014. Different from SWR's ZMD, the initial central feature of TWR was located in LH, but it moved to ZMD during 2004–2009. Subsequently, SWR and TWR moved to PDS simultaneously in 2010–2014, and moved back to ZMD in 2015–2019. In addition, the mean centers of SWR and TWR fluctuated significantly during this period (2010–2014), while the mean center of GWR fluctuated less.

As shown in Figure 5, the Global Moran's I values of all three indicators were greater than 0, at 0.342, 0.287, and 0.072, respectively, indicating that they did not have a random spatial distribution. However, the Global Moran's I of TWR was very close to 0, and the *p*-value and *z*-score caused it to fail the hypothesis test. Thus, the analysis results were presented as a random distribution in the figure, or its clustering was not significant enough, which will be discussed later with the Local Moran's I. Meanwhile, both SWR and GWR showed spatial clustering characteristics, with a *p*-value and *z*-score of 0.014 and 2.444 and 0.059 and 1.887, respectively. SWR had a higher degree of clustering than GWR because SWR passed the 95% significance test, while GWR passed the 90% significance test. Perhaps because TWR is a synthesis of SWR and GWR, geographical clustering features are not as intuitive.

The hot spots of SWR, GWR, and TWR were all distributed in Nanyang city and Xinyang city in the southwest of Henan Province, as shown in Figure 6(a). The other regions had neither hot spots nor cold spots, showing insignificant properties. The confidence levels of SWR and TWR were the same, while the confidence levels of GWR hot spot analysis were relatively lower. The Local Moran's I of GWR showed that Zhengzhou City and Anyang city had low–low clusters, while the rest of the regions were insignificant. The results of SWR and TWR were consistent. Zhengzhou city, Xinxiang city, and Anyang city are

Table 1 | Multiyear water resource statistics by the time period (unit: billion m^3)

	1999–2004			2005–2009			2010–2014			2015–2019		
City	SWR	GWR	TWR	SWR	GWR	TWR	SWR	GWR	TWR	SWR	GWR	TWR
Zhengzhou	0.647	1.006	1.309	0.512	0.882	1.068	0.478	0.847	0.935	0.391	0.633	0.794
Kaifeng	0.431	0.833	1.175	0.483	0.801	1.179	0.375	0.683	0.957	0.339	0.721	0.92
Luoyang	1.895	1.198	2.325	1.825	1.306	2.172	2.483	1.287	2.799	1.469	1.15	1.756
Pingdingshan	1.998	0.84	2.485	1.471	0.786	1.913	1.523	0.688	1.905	0.86	0.576	1.186
Anyang	0.501	0.958	1.17	0.534	0.848	1.139	0.406	0.815	0.993	0.495	0.812	1.076
Hebi	0.128	0.31	0.368	0.155	0.268	0.353	0.114	0.237	0.29	0.11	0.223	0.265
Xinxiang	0.527	1.257	1.432	0.55	1.097	1.402	0.436	1.076	1.238	0.391	1.004	1.111
Jiaozuo	0.345	0.603	0.792	0.397	0.546	0.839	0.34	0.572	0.797	0.315	0.522	0.734
Puyang	0.225	0.652	0.7	0.251	0.565	0.645	0.212	0.536	0.565	0.117	0.513	0.431
Xuchang	0.411	0.739	1.021	0.417	0.666	0.936	0.324	0.576	0.765	0.255	0.513	0.693
Luohe	0.346	0.435	0.754	0.291	0.374	0.62	0.193	0.359	0.524	0.159	0.36	0.482
Sanmenxia	1.339	0.592	1.466	1.327	0.575	1.435	1.623	0.661	1.751	1.108	0.67	1.211
Nanyang	6.146	2.353	7.171	6.584	2.269	7.443	5.78	2.176	6.689	3.573	2.189	4.547
Shangqiu	0.792	1.489	2.224	0.567	1.421	1.953	0.428	1.203	1.587	0.596	1.064	1.618
Xinyang	7.997	2.856	8.967	7.735	2.871	8.481	4.699	2.264	5.388	7.369	2.661	7.893
Zhoukou	1.36	1.77	2.883	1.307	1.941	2.925	0.883	1.686	2.218	0.753	1.582	2.103
Zhumadian	3.711	2.164	5.41	4.646	2.21	6.06	1.693	1.71	2.818	2.807	2.1	4.026
Jiyuan	0.226	0.199	0.303	0.277	0.196	0.349	0.237	0.271	0.32	0.204	0.194	0.282

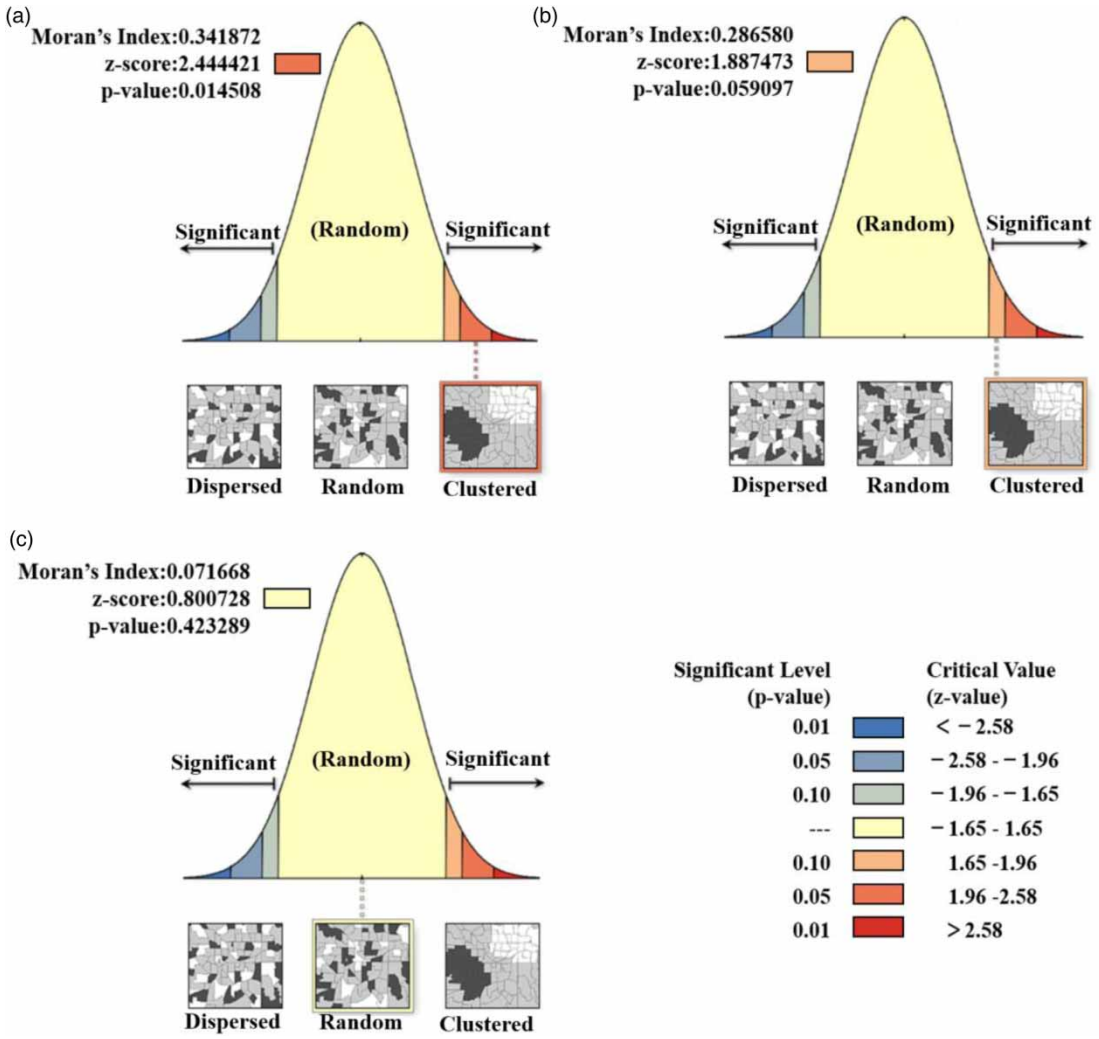

Figure 5 | Results of the Global Moran's I analysis of (a) SWR, (b) GWR, and (c) TWR.

low–low clusters, while the rest of the regions were insignificant. In addition, there were no spatial anomalies in the three indicators over the 21 years (Figure 6(b)). It is worth mentioning that although TWR did not show clustering characteristics in the Global Moran's I, there were still low–low clusters in the local Moran's I.

Temporal variation in water resources

According to the results of the M-K trend and mutation tests and the confidence map of the two-tailed tests shown in Figure 7(a), no more than half of the cities had a significant change trend, and all had a decreasing trend since their *z*-values were less than 0. The results of SWR, GWR, and TWR were similar, and the cities with significant trends were all distributed in central and northeastern Henan Province, among which cities with change trends in GWR were the most significant and numerous. GWR and TWR passed the significance test in 9 and 7 cities, respectively, with a maximum confidence level of 99%, while the 5 cities of SWR passed only the test with a confidence level of 90%. In addition, based on a province-wide perspective, the M-K results showed that none of the three indicators had a significant change trend.

Abrupt changes in the same dataset were analyzed using the M-K method, and the significance level was taken as 0.1. Since the time series data were available only for 21 years, abrupt changes may not be clearly observed, and only a few cities with more obvious abrupt changes were listed in this paper. In the SWR time series, the abrupt changes occurred in approximately 2011 in AY, KF, and ZMD and in approximately 2012, 2013, and 2014 in PDS, LH, and PY, respectively, while two abrupt changes occurred in XY in 2008 and 2015. In the GWR time series, only XY, HB, LH, and PDS had abrupt changes. Xinyang

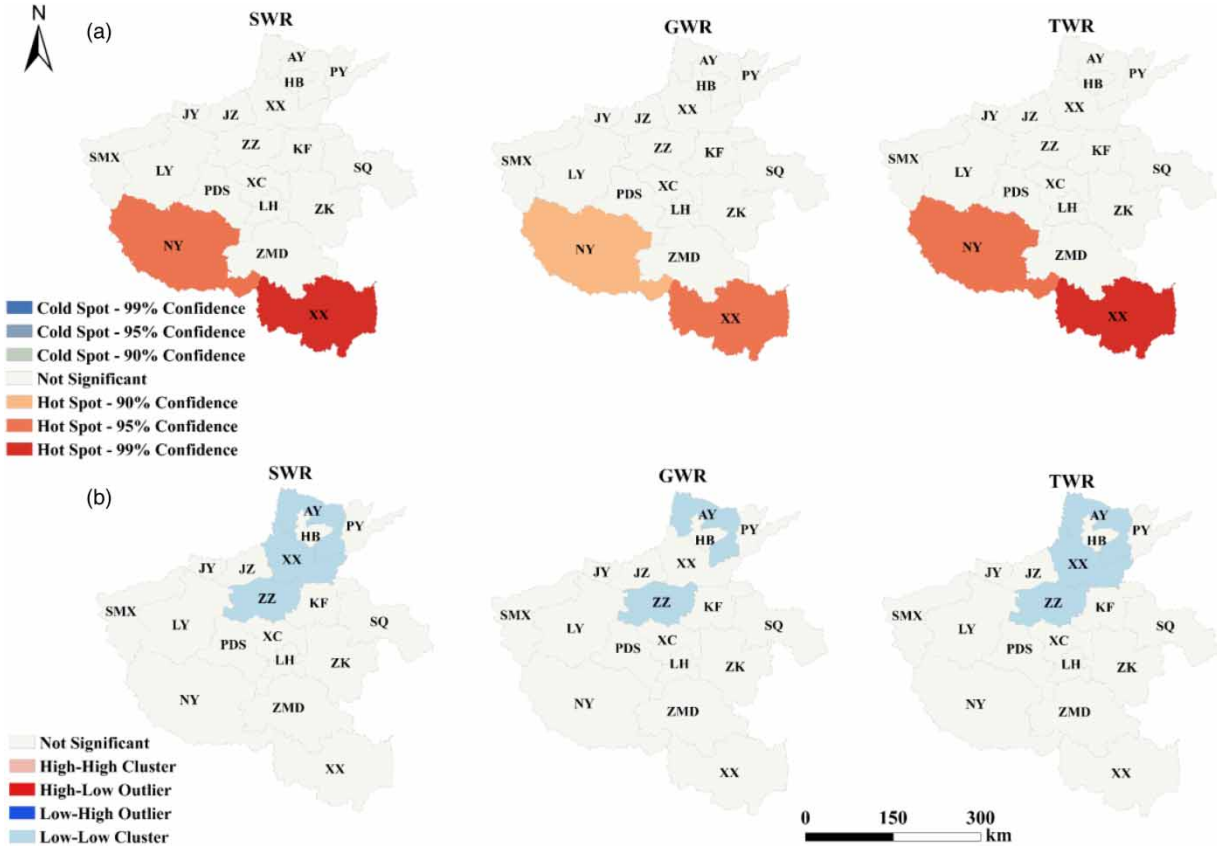

Figure 6 | The results of (a) hot spot analysis and (b) Local Moran's I.

had two mutations in 2008 and 2015, while the mutations in the other three cities occurred in approximately 2010, 2011, and 2012. For TWR, abrupt changes occurred in 2009 in ZMD, in 2010 in SQ and ZK, in 2011 in AY and KF, in 2012 in HB and PDS, and in 2013 in PY and ZZ, and two abrupt changes occurred in 2008 and 2015 in XY. Based on the provincial perspective, the abrupt changes of SWR, GWR, and TWR all occurred in approximately 2011.

Comparing the fitting results of several schemes, this paper divided 21 years of water resource data into four subintervals and calculated Hurst exponent (H) for each city and for the entire province. The results are shown in Figure 7(b). The H of GWR was concentrated mainly in the greater than 0.5 interval, showing persistence, but the persistence of GWR in some cities was slightly weaker; even in some areas of southern Henan, H was less than 0.5. The H-values of SWR and TWR were concentrated mainly in the less than 0.5 interval, indicating inverse persistence. Compared with SWR, the H of TWR was closer to 0.5, which means that its inverse persistence is weaker. In other words, for GWR, most cities had the same trend in the future as in the past, while for SWR and TWR, most cities had an opposite trend in the future than that in the past.

Based on the province-wide perspective, the H-values for SWR, GWR, and TWR were 0.52, 0.83, and 0.58, respectively, which were all greater than 0.5. Therefore, these series were all considered to be persistent, but the persistence of SWR and TWR was weaker and much lower than that of GWR. This means that the future trend of GWR will be consistent with the past trend with a high probability, while the future trends of SWR and TWR will be consistent with the past with a low probability. Combining the results with the individual R/S analysis of each city, we can conclude that GWR has obvious persistence, while SWR and TWR do not have obvious persistence or have inverse persistence.

Analysis of influencing factors

The temperature data from 17 meteorological stations in Henan Province were interpolated to obtain the annual average temperature of the province as well as the average temperature in each city. The annual average temperature in Henan

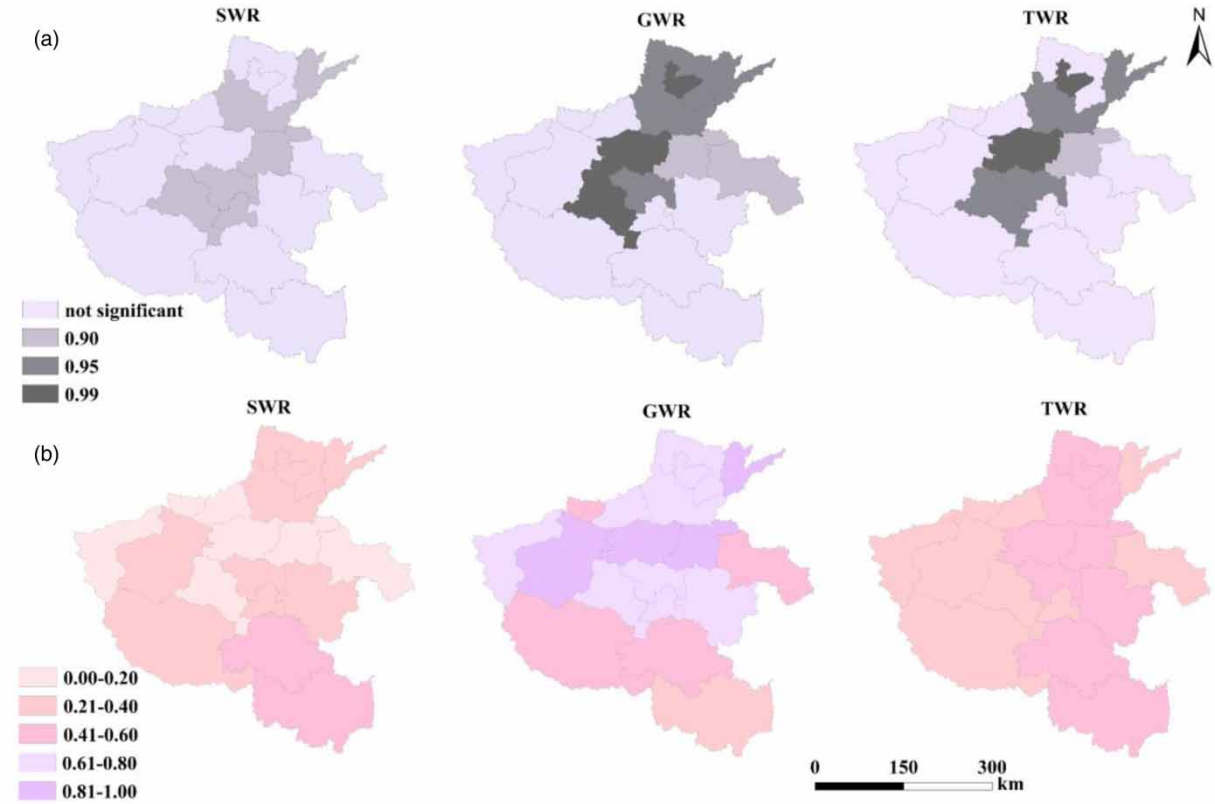

Figure 7 | (a) Confidence level of the trend test and (b) Hurst value distribution of water resources.

Province reached its lowest point within a decade in approximately 2011. The M-K method showed that the temperature and precipitation in Henan Province changed abruptly in approximately 2012 and 2011, respectively. The general trend of the temperature change in each city during this 21-year period was similar to that at the provincial scale. In terms of time, the temperature and precipitation coincided with the mutation time of water resources mentioned above. In terms of space, the geographical distribution of the temperature and precipitation decreased from south to north, which was somewhat consistent with the geographical distribution of water resources described in the above section.

SPSS (Statistical Product Service Solutions) is a series of software used in statistical analysis and calculation, data mining, and so on. The correlation between climatic factors and water resource series was determined with linear regression analysis in SPSS software, and the results are shown in Table 2. These two climate factors were significantly correlated with water resources, among which water resources are negatively correlated with temperature and positively correlated with precipitation. The correlation passed the significance test, so the results are reliable. However, the correlation between water resources and temperature was much lower than that of precipitation, with the R^2 between temperature and water resources being approximately 0.35, while the R^2 between precipitation and water resources reached approximately 0.9. On the one hand, temperature affects water resources by influencing the degree of evapotranspiration, especially of surface water, and on the other hand, it can affect water resources by influencing precipitation. Precipitation falls to the ground to form surface runoff or infiltrates to become subsurface runoff, and it is one of the main sources of water resources. In contrast, precipitation has a more direct impact on water resources. Considering that the positive effect of precipitation on water resources is much greater than the negative effect of temperature on water resources, the decreasing water resources from south to north are well understood.

Geographically, cropland is distributed mainly in the central and eastern parts of Henan Province, forest is distributed mainly in the western part of Henan Province, water is distributed mainly in the southwest part of Henan Province, and settlement is distributed mainly in several central and northern cities with Zhengzhou at the center. In the past 20 years, the areas of arable land, grassland, and undeveloped land have gradually decreased, while the areas of water and construction land has gradually increased, and the area of forestland has been maintained at approximately 16.25%. However, as a large

Table 2 | Results of the correlation analysis of climate and land use and water resources

	SWR		GWR		TWR	
	r	sig	*r*	sig	*r*	sig
Temperature	−0.595**	0.004	−0.567**	0.007	−0.598**	0.004
Precipitation	0.946**	0.000	0.966**	0.000	0.959**	0.000
Cropland	0.299	0.188	0.331	0.143	0.344	0.127
Forest	−0.016	0.946	−0.088	0.704	−0.071	0.760
Grassland	0.192	0.405	0.248	0.279	0.245	0.285
Other	−0.032	0.892	0.064	0.783	0.031	0.895
Settlement	−0.312	0.169	−0.342	0.130	−0.356	0.113
Water	−0.095	0.682	−0.140	0.545	−0.141	0.541
Wetland	0.292	0.199	0.340	0.132	0.336	0.136

**The correlation is significant at the 0.01 level (two-tailed); *r* denotes the Pearson correlation coefficient; sig denotes the significance of the two-tailed test.

agricultural province, the proportion of arable land in Henan Province has always been greater than 70%. The land use change matrix calculated by ArcGIS from 1999 to 2019 is organized as follows (Table 3).

The correlation between each land cover area and the amount of water resources was determined using SPSS based on 21 years of land use data (Table 2), and the results showed that there was no significant correlation between each land use type and water resources. Different land use types have different underlying surfaces that affect the infiltration process and surface runoff. SWR is mainly natural river runoff, and the change in land use type may briefly affect the SWR at that time, but from the annual scale, land use type has had little impact on surface water resources, which is understandable. Similarly, land use has little impact on GWR and TWR. However, we cannot completely eliminate the impact of human activities such as land use on water resources, and this topic requires more detailed data for further research.

CONCLUSIONS

In this paper, through the analysis of the spatial and temporal distribution characteristics and influencing factors of water resources in Henan Province, the following conclusions were drawn.

Based on the analysis results of available information, we concluded that the spatial distribution and statistical characteristics of SWR were relatively similar to those of TWR. In the past 21 years, the water resources in Henan Province have been declining. Based on the statistical examination, XY, NY, and ZMD in the southeastern of Henan Province have abundant water resources, while several cities in the northeast have lower water resources.

The time period from 2010 to 2014 showed a clear spatial fluctuation in water resources with a tendency to migrate northward, especially in SWR and TWR. The time series of water resources also showed a mutation, and the time was concentrated

Table 3 | Land use transfer matrix from 1999 to 2019

2019 \ 1999	Cropland	Forest	Grassland	Other	Settlement	Water	Wetland	Total
Cropland	77.79512%	0.08518%	0.07159%	0.00284%	0	0.00185%	0	77.95657%
Forest	0.48577%	14.17116%	0.10628%	0.09133%	0	0.00161%	0.00033%	14.85648%
Grassland	0.03069%	0.00292%	0.27080%	0	0	0.00385%	0	0.30826%
Other	0.00052%	0.00103%	0	0.07119%	0	0	0	0.07275%
Settlement	4.65981%	0.00253%	0.12357%	0.00029%	0.99216%	0.00067%	0.01201%	5.79102%
Water	0.10304%	0.00094%	0.00998%	0	0	0.60100%	0.00501%	0.71998%
Wetland	0.00010%	0.00010%	0.00005%	0	0	0.00237%	0.29233%	0.29494%
Total	83.07503%	14.26386%	0.58226%	0.16565%	0.99216%	0.61135%	0.30969%	100.00000%

from 2008 to 2015. In addition, three cities, PDS, ZMD, and KF, showed a more obvious sudden temporal change in the water resource time series.

Combining the M-K nonparametric test and the R/S analysis method, it is clear that in the GWR time series, cities that have had a decreasing trend in the past will also continue to decline in the future, while several cities in the SWR and TWR series that have had a decreasing trend in the past will have the opposite upward trend in the future.

Among the factors influencing water resources, precipitation had the greatest degree of influence on water resources, followed by temperature, while land use type had no significant influence on water resources. Accordingly, the temporal variation in climate factors could reasonably explain the variation in water resources over the past 21 years.

DATA AVAILABILITY STATEMENT

All relevant data are included in the paper or its Supplementary Information.

FUNDING STATEMENT

This study was funded by the Science and Technology Project in Henan Province (232102320026 and 232102320032), the National Natural Science Foundation of China (Grant Nos. 51509222 and 51909091) and Project of China Geological Survey (NO.DD20211256).

CONFLICT OF INTEREST

The authors declare there is no conflict.

REFERENCES

Bhatti, A. Z., Farooque, A. A., Li, Q., Abbas, F. & Acharya, F. 2021 Spatial distribution and sustainability implications of the Canadian groundwater resources under changing climate. *Sustainability* **13** (17), 9778.

Deng, D., Zhao, Z. B. & Ma, Y. 2020 Modeling of species distribution with GIS in arid regions: take Caragana korshinskii for example. *Journal of Desert Research* **40** (05), 74–80.

Du, Q. H. & Song, Q. X. 2021 Study on overexploitation of groundwater in Henan Province and control measures. *Water Resources Development and Management* **01**, 33–37.

Freund, E. R., Abbaspour, K. C. & Lehmann, A. 2017 Water resources of the Black Sea Catchment under future climate and landuse change projections. *Water* **9** (8), 598.

Gu, W., Wang, J. & Zhu, L. 2010 Changes in precipitation and water resources in Henan Province in 1956–2007. *Advances in Climate Change Research* **6** (4), 277–283.

He, L., Xu, L., Lu, H. W., Feng, W. & Shi, R. K. 2021 Characteristics of nitrogen balance transformation in farmland of Yangtze River Economic Belt from 1990 to 2018. *China Environmental Science* **41** (10), 4820–4828.

Khan, M. Y. A., Gani, K. M. & Chakrapani, G. J. 2017 Spatial and temporal variations of physicochemical and heavy metal pollution in Ramganga River – a tributary of River Ganges, India. *Environmental Earth Sciences* **76**, 231.

Khan, M. Y. A., Hu, H., Tian, F. & Wen, J. 2020 Monitoring the spatio-temporal impact of small tributaries on the hydrochemical characteristics of Ramganga River, Ganges Basin, India. *International Journal of River Basin Management* **18** (2), 231–241.

Li, T., Qiu, S., Mao, S., Bao, R. & Deng, H. 2019 Evaluating water resource accessibility in southwest China. *Water* **11** (8), 1708.

Liu, J. Y., Qin, K. Y., Zhen, L., Xiao, Y. & Xie, G. D. 2020 How to allocate interbasin water resources? A method based on water flow in water-deficient areas. *Environmental Development* **34** (1), 100460.

Peng, J., Liu, Z. H., Liu, Y. H., Wu, J. S. & Han, Y. N. 2012 Trend analysis of vegetation dynamics in Qinghai–Tibet Plateau using Hurst Exponent. *Ecological Indicators* **14** (1), 28–39.

Qi, H. 2019 The application of R/S and Mann-Kendall methods in groundwater management model in Jinan City. *China Rural Water and Hydropower* **08**, 20–25.

Rahmani, J. & Danesh-Yazdi, M. 2022 Quantifying the impacts of agricultural alteration and climate change on the water cycle dynamics in a headwater catchment of Lake Urmia Basin. *Agricultural Water Management* **270**, 1–14.

Song, M. L., Wang, R. & Zeng, X. Q. 2018 Water resources utilization efficiency and influence factors under environmental restrictions. *Journal of Cleaner Production* **184**, 611–621.

Wang, X. X., Xiao, X. M., Zou, Z. H., Dong, J. W., Qin, Y. W., Doughty, R. B., Menarguez, M. A., Chen, B. Q., Wang, J. B., Ye, H., Ma, J., Zhong, Q. Y., Zhao, B. & Li, B. 2020 Gainers and losers of surface and terrestrial water resources in China during 1989–2016. *Nature Communications* **11** (1), 3471.

Wang, D. G., Yu, M., Mo, W., Lv, D.-A., Cheng, J. & Sun, L. 2021 Ecological safety evaluation for water resources of China based on pressure-state-response model: a case from Zhoushan archipelago. *Nature Environment and Pollution Technology* **20** (2), 601–612.

Wei. 2007 *Modern Climate Statistical Diagnosis and Prediction Techniques*. China Meteorological Press, Beijing.

Xiao, Y., Li, W. J. & Yang, S. F. 2019 Changing temporal and spatial patterns of fluvial sedimentation in Three Gorges Reservoir, Yangtze River, China. *Arabian Journal of Geosciences* **12** (15), 490.

Yang, J. Y., Zhao, C., Liu, G. S. & Xu, Y. 2017 Mann-Kendall and R/S methods combined-analysis on changing trend of hydrological series – a case of Suzhou. *Water Resources and Hydropower Engineering* **48** (02), 27–30, + 137.

Ye, X. C., Xu, C.-Y., Li, X. H. & Zhang, Q. 2018 Comprehensive evaluation of multiple methods for assessing water resources variability of a lake-river system under the changing environment. *Nordic Hydrology* **49** (1–2), 332–343.

Yu, L., Guo, J. H. & Wang, H. L. 2021 Harmonious evaluation of regional water-energy-food coupling system. *South-to-North Water Transfers and Water Science & Technology* **19** (03), 437–445.

Zhang, H. D., Wei, W. & Xue, S. 2015 Analysis on the variation of temperature and precipitation in Dingxi based on R/S and Mann-Kendall Test. *Research of Soil and Water Conservation* **22** (06), 183–189.

Zhang, W. Q., Du, J. H., Wang, Y. X., Li, J. Y., Feng, P., Sun, H., Qiao, G. D., Sun, X. L. & Li, S. 2020 Bottlenecks facing protection and utilization of water resources in Henan province and the solutions to resolve them. *Journal of Irrigation and Drainage* **39** (10), 123–129.

Zhao, Q. H., Ding, S. Y., Ji, X. Y., Hong, Z. D., Lu, M. W. & Wang, P. 2021 Relative contribution of the Xiaolangdi Dam to runoff changes in the lower Yellow River. *Land* **10** (5), 521.

Zhou, J. C. 2014 The balance analysis and forecast on supply and demand of water resources in Henan based on Grey Model. *Journal of Zhongyuan University of Technology* **25** (03), 57–62, + 70.

Zuo, Q. T., Li, W., Zhao, H., Ma, J. X., Han, C. H. & Luo, Z. L. 2020 A harmony-based approach for assessing and regulating human-water relationships: a case study of Henan Province in China. *Water* **13** (1), 32.

First received 9 September 2022; accepted in revised form 24 February 2023. Available online 17 March 2023